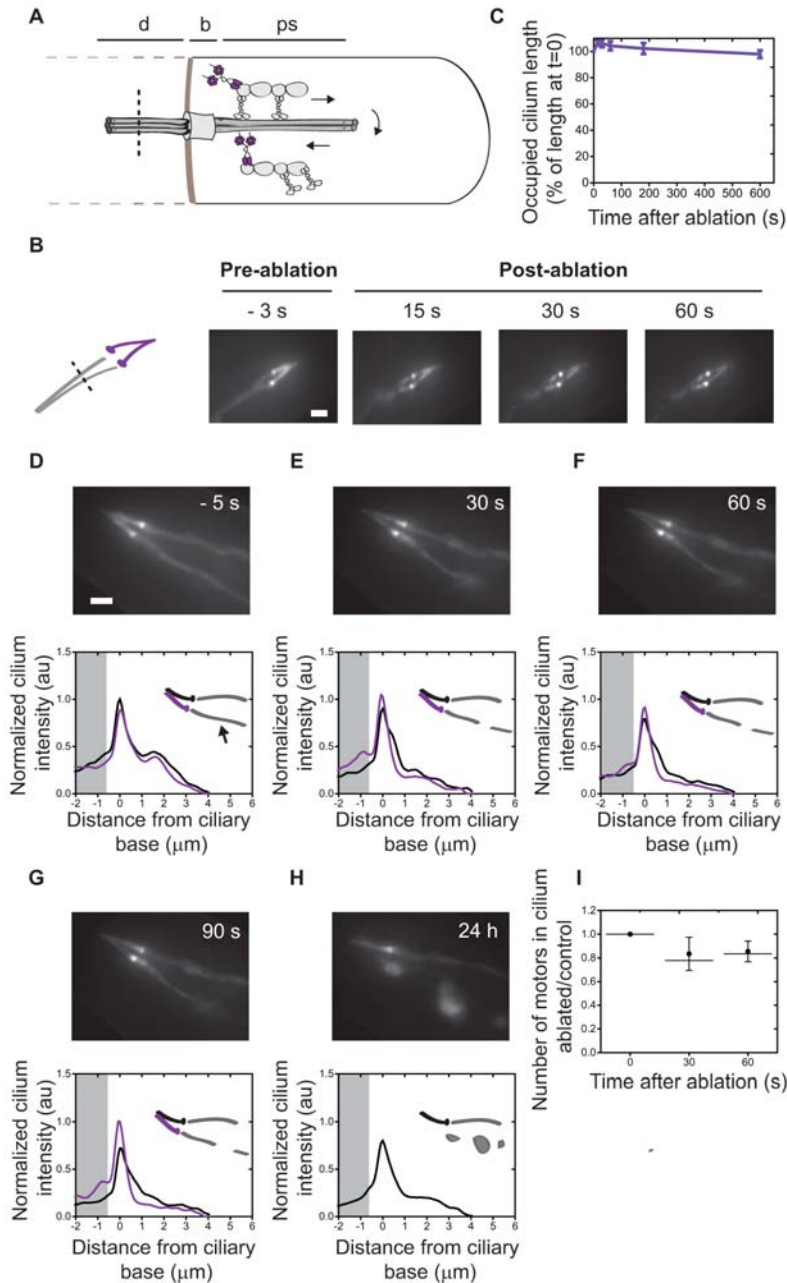


# Supplemental Materials

*Molecular Biology of the Cell*

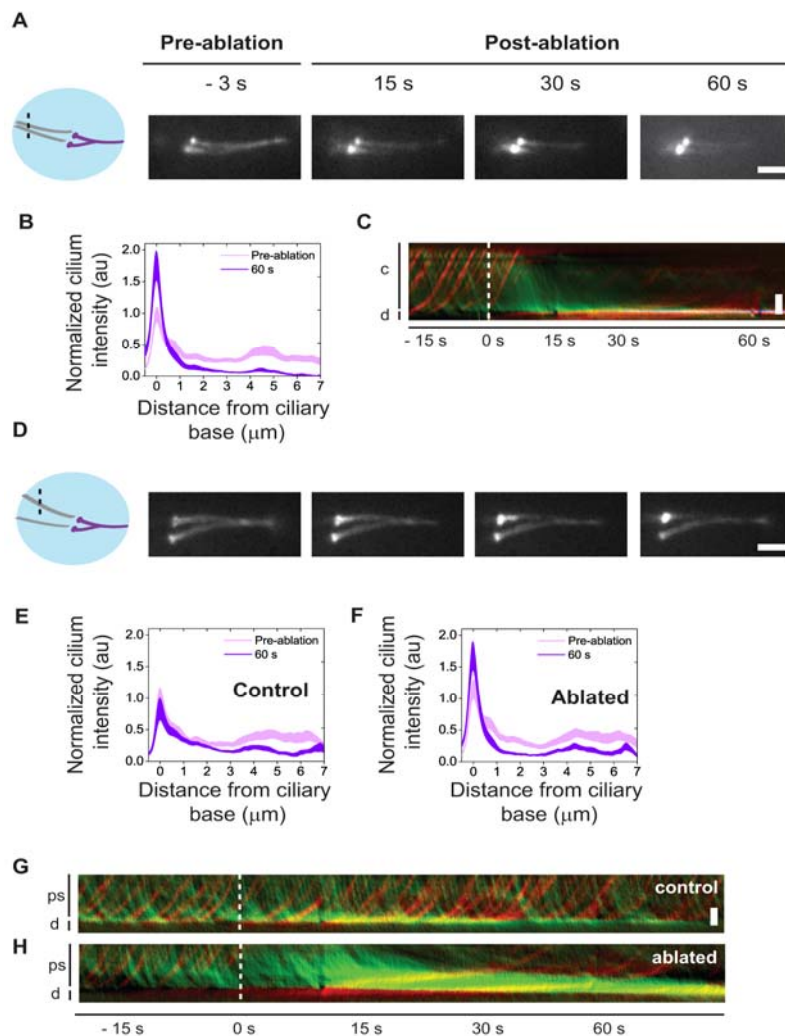
Mijalkovic et al.



Supplemental Figure 1

Stability of the proximal segment and IFT dynein redistribution in *osm-3* mutant background worms. (A) Cartoon schematic of intraflagellar transport (IFT) inside the cilium in *osm-3* worms, which lack the distal segment. d: dendrite; b: base; ps: proximal segment; tan: periciliary diffusion barrier; dotted tan line: periciliary membrane; dotted grey line: cell membrane; dotted black line: position of laser cut. (B) Left: cartoon showing position of dendritic laser ablation (dotted line). Right: representative summed fluorescence intensity images of IFT dynein (XBX-1::EGFP) in the dendrite and phasmid cilium pre- and post-ablation. (C) IFT

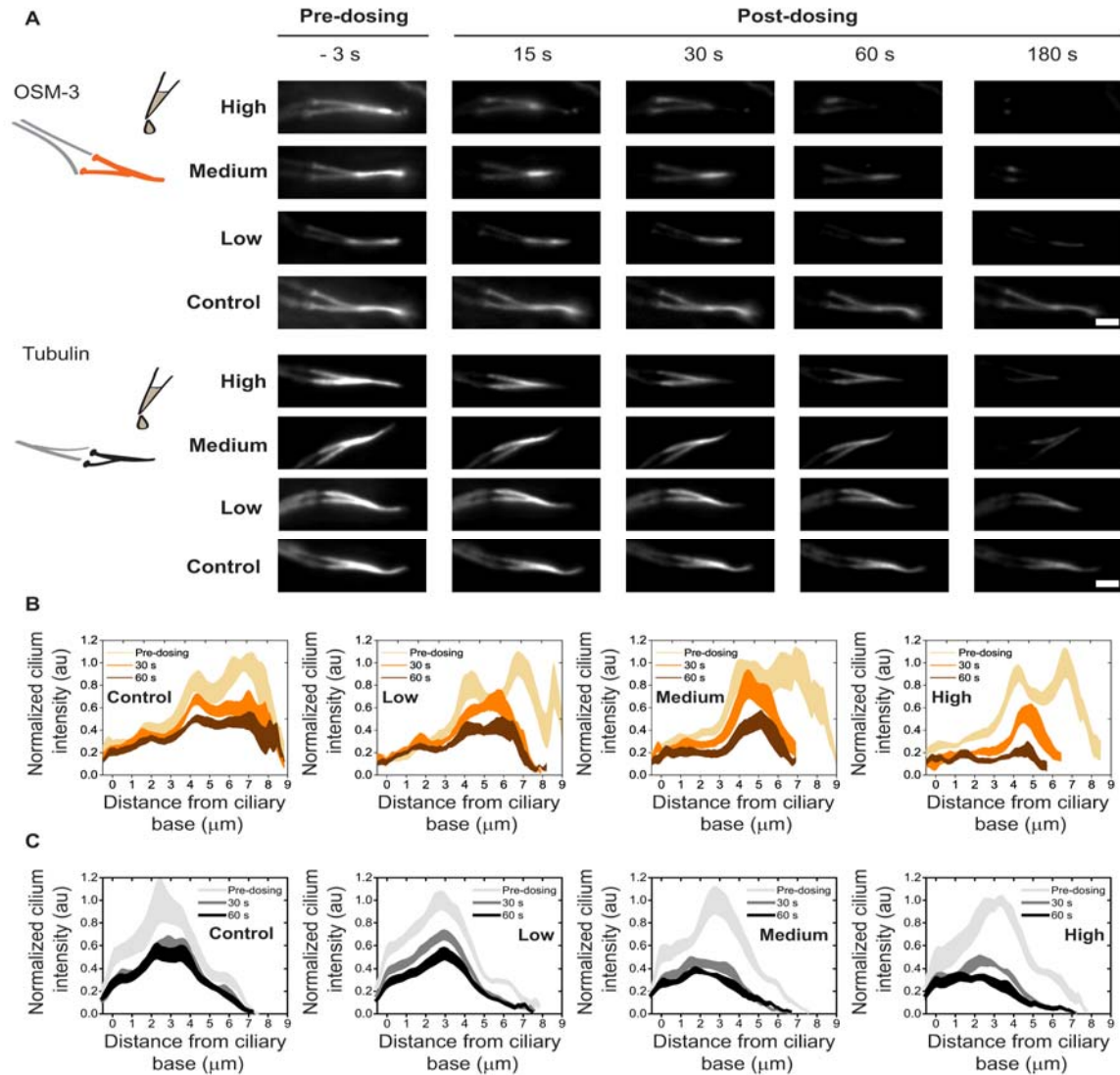
dynein (n=17) retraction as percentage of pre-ablation occupied ciliary distance. Error is s.e.m. (D-H) XBX-1::EGFP representative summed fluorescence images and cilium intensity pre-ablation (D) and 30 s (E), 60 s (F), 90 s (G) and 24 hours (H) post-ablation of the ablated and non-ablated (control) cilium in *osm-3* worms. Grey area indicates the dendrite. Scale bar: 2  $\mu\text{m}$ . (I) Ratio of ablated/control XBX-1 number in the cilium pre- and post-ablation in the *osm-3* mutant background. Dot, average; error bar, 95% confidence interval; line, median.



### Supplemental Figure 2

Primary response of IFT dynein to dendritic femtosecond-laser ablation of EGTA-treated worms. (A, D) Left: cartoon showing position of the focus of the ablation laser (dotted line) in EGTA-treated (turquoise) worms. (A) Right: Representative

summed fluorescence intensity images of IFT dynein (XBX-1::EGFP) in the phasmid cilium, pre- and post-ablation. Scale bar: 2  $\mu\text{m}$ . (B) Averaged, normalized cilium fluorescence 3 s pre-ablation and 60 s post-ablation of IFT dynein (purple,  $n = 14$  cilia from 14 worms). Line thickness is s.e.m. (C) Representative IFT dynein kymograph showing retrograde (green) and anterograde (red) motility. Horizontal: time; vertical: position; c, cilium; d, dendrite; scale bar: 2  $\mu\text{m}$ . Moment of ablation is indicated by the dotted line. (D) Right: Representative summed fluorescence intensity images of IFT dynein (XBX-1::EGFP) in the phasmid cilium, pre- and post-ablation. Bottom cilium: non-ablated dendrite, control. Top cilium: ablated dendrite. Scale bar: 2  $\mu\text{m}$ . (E-F) Averaged, normalized cilium fluorescence 3 s pre-ablation and 60 s post-ablation ( $n = 8$  cilia from 8 worms). Line thickness is s.e.m. (G-H) Representative IFT dynein kymograph showing retrograde (green) and anterograde (red) motility in the proximal segment of cilia with control (G) and ablated (H) dendrite. Horizontal: time; vertical: position; d, dendrite; ps, proximal segment; scale bar: 1  $\mu\text{m}$ . Moment of ablation is indicated by the dotted line.



### Supplemental Figure 3

The effect of ATP depletion on OSM-3 and the ciliary axoneme. (A) Left: cartoons showing sodium azide treatment. Right: Representative summed fluorescence intensity images of OSM-3 (OSM-3::mCherry) and tubulin (TBB-4::EGFP) in the phasmid cilium, pre- and post-dosing. Scale bar: 2  $\mu\text{m}$ . (B) Averaged, normalized cilium fluorescence of OSM-3 pre- and post-dosing in control (M9-treated) worms ( $n = 8$  worms, 8 cilia) and azide-treated worms at low ( $n = 7$  worms, 7 cilia), medium ( $n = 13$  worms, 13 cilia) and high ( $n = 8$  worms, 9 cilia) concentration. Pre-dosing, light orange; 30 s post-dosing, orange; 60 s post-dosing, brown. Line thickness is s.e.m. (C) Averaged, normalized cilium fluorescence of TBB-4 pre- and post-dosing in control (M9-treated) worms ( $n = 7$  worms, 7 cilia) and azide-treated worms at low ( $n = 9$  worms, 10 cilia), medium ( $n = 11$  worms, 11 cilia) and high ( $n = 7$  worms, 7 cilia) concentration. Pre-dosing, light grey; 30 s post-dosing, grey; 60 s post-dosing, black. Line thickness is s.e.m.